

Sign and Magnitude Tunable Coupler for Superconducting Flux Qubits

R. Harris,* A. J. Berkley, M. W. Johnson, P. Bunyk, S. Govorkov, M. C. Thom, S. Uchaikin, A. B. Wilson, J. Chung, E. Holtham, J. D. Biamonte, A. Yu. Smirnov, M. H. S. Amin, and A. Maassen van den Brink[†]
D-Wave Systems Inc., 100-4401 Still Creek Dr., Burnaby, BC V5C 6G9, Canada[‡]

(Dated: December 2, 2024)

We report experimental results confirming the functionality of a coupling element for flux based superconducting qubits, with a coupling strength J whose sign and magnitude can be tuned *in situ*. To measure the effective J we map the groundstate of a coupled two qubit system as a function of the local magnetic fields applied to each qubit. These measurements demonstrate that J can be tuned from antiferromagnetic through zero to ferromagnetic.

PACS numbers: 85.25.Dq, 03.67.Lx

One approach to building useful quantum computer processors is to abandon the gate model in favor of physics-inspired quantum computational models, such as adiabatic quantum computation (AQC) and its variants [1]. Realistic processor architectures based on the AQC model exist [2, 3], and are well-suited to quickly producing accurate approximate solutions to NP-complete problems [4]. One such AQC processor architecture, based on superconducting electronics [5, 6, 7, 8], requires superconducting devices that can pairwise couple qubits with *in situ* programmable coupling magnitude and sign [9, 10]. In this letter we adopt a known superconducting flux qubit design and focus on an experimental demonstration of a sign and magnitude programmable coupling element between two such flux qubits.

The qubit design used is a bistable rf-SQUID that is magnetically biased near its degeneracy point by an externally applied flux $\Phi_x = \Phi_0/2$ (where $\Phi_0 = h/2e$ is the flux quantum) as described in Refs. [11, 12, 13, 14, 15]. The qubits are represented by loops a and c in Fig. 1 with external bias controls ϕ_x^a and ϕ_x^c (where $\phi_x^i \equiv 2\pi\Phi_x^i/\Phi_0$ is a phase parameter and Φ_x^i represents the flux applied to element i). In addition, compound junctions with separate flux bias controls are employed in the rf-SQUIDs to facilitate tuning of the critical current I_c^i ($i = a, c$) of the qubits [16, 17]. These components are represented in Fig. 1 as loops d and e with external bias controls ϕ_x^d and ϕ_x^e . It has been established that one can obtain either ferromagnetic or antiferromagnetic coupling between two flux qubits by simply placing them in close proximity and tailoring their geometry [18]. However this approach can only provide coupling of fixed magnitude and sign. Tunable coupling requires a third device fabricated between the two qubits [19, 20, 21, 22, 23, 24]. We have chosen to implement such a coupler using a monostable rf-SQUID with separate bias control, as proposed in Ref. [20]. This element is represented by loop b with bias control ϕ_x^b in Fig. 1. To our knowledge this and the work reported in [21] are the first successful demonstrations of a coupler between superconducting flux qubits capable of being tuned *in situ* to produce ferromagnetic, antiferromagnetic and zero coupling.

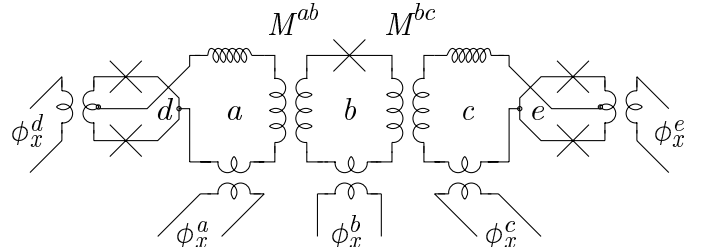


FIG. 1: Device schematic. Loops a and c are the rf-SQUID qubits with bias controls ϕ_x^a and ϕ_x^c . Loop b is the rf-SQUID coupler with bias control ϕ_x^b . Loops d and e are the compound junctions, controlled by biases ϕ_x^d and ϕ_x^e .

We couple two qubits into the rf-SQUID coupler loop via transformers leading to mutual inductances M^{ab} and M^{bc} so that the qubits are influenced by the persistent current in the coupler $I_p^b = \langle I_c^b \sin(\phi^b) \rangle$, not the applied control flux Φ_x^b . A change in the persistent current in one of the qubits I_p^q will drive a change in I_p^b proportional to the coupler's dc susceptibility $\chi^b \equiv dI_p^b/d\Phi_x^b$, which will then alter the net flux applied to the second qubit. Since χ^b is a periodic function whose sign changes as a function of Φ_x^b , the resultant qubit-qubit interaction can be ferromagnetic ($\chi^b < 0$), antiferromagnetic ($\chi^b > 0$), or zero.

Since the effective bandwidth of the coupler is set by the energy spacing between its ground and first excited states, we designed this to be much higher ($\gg 10$ GHz) than the typical energy splitting between qubit states in our implementation. As such, the effective low energy Hamiltonian for the composite qubit-coupler-qubit system contains only 4 states:

$$\begin{aligned} \mathcal{H} &= \sum_{q=a,c} \mathcal{H}^q + \mathcal{H}^{co} \\ &= - \sum_{q=a,c} \left(\epsilon^q \sigma_z^{(q)} + \Delta^q \sigma_x^{(q)} \right) + J(\phi_x^b) \sigma_z^{(a)} \sigma_z^{(c)} \quad (1) \end{aligned}$$

where $\sigma_x^{(q)}$ and $\sigma_z^{(q)}$ are Pauli matrices acting on the state of qubit q and the Hamiltonian of the individual qubits \mathcal{H}^q has been described in Ref. [11]. The term \mathcal{H}^{co} de-

scribes the interaction term governed by the coupler. Let the magnitudes of the persistent currents in the qubit states be I_p^a and I_p^c . The local qubit biases $\epsilon^q \propto \phi_x^q I_p^q$ ($q = a, c$) and effective qubit-qubit coupling [20]

$$J = M^{ab} M^{bc} \chi^b I_p^a I_p^c = M^{ab} M^{bc} I_p^a I_p^c \frac{dI_p^b}{d\Phi_x^b} \quad (2)$$

all scale with I_p^a and I_p^c . In turn, we expect I_p^q and the qubit tunneling energy Δ^q to be functions of the compound junction biases ϕ_x^d and ϕ_x^e on qubits $q = a$ and c , respectively.

The qubits and coupler were fabricated on an oxidized silicon wafer using a niobium trilayer process with wiring layers isolated by a sputtered SiO_2 dielectric. The inductance of the rf-SQUID qubits was designed to be 500 pH. The two junctions making up each compound junction were designed to have a total parallel capacitance of $C^q = 20$ fF. An independent measure of the qubit capacitance for a similar device through fitting of macroscopic resonant tunneling peaks [25] at large I_p^q yielded $C^q = 33 \pm 3$ fF. We suggest that the discrepancy is due to capacitive loading of the junction by nearby wiring. The unsuppressed I_c^q ($q = a, c$) of each compound junction was designed to be $1.25 \mu\text{A}$. The coupler is a single junction rf-SQUID with designed inductance $L^b = 240$ pH and $I_c^b = 0.9 \mu\text{A}$, which can be expressed as $\beta^b \equiv 2\pi L^b I_c^b / \Phi_0 = 0.65$. Fits to the measured flux generated by the coupler's persistent current as detected by each of the qubits (explained below) yielded $\beta^b = 0.63 \pm 0.02$. The mutual inductance between the coupler and qubits was designed to be $M^{ab} = M^{bc} \equiv M^{qb} = 25$ pH. Measurements on similar breakout structures yielded $M^{qb} = 28 \pm 2$ pH.

For readout purposes we inductively couple each qubit to its own dedicated hysteretic dc-SQUID [26, 27]. When there is no flux applied to the qubit compound junctions (I_p^q maximized) we are able to distinguish between the two flux states of each qubit.

The device was mounted in an aluminum box in a dilution refrigerator with base temperature below 10 mK. The sample area was located inside two coaxial cryoperm shields and the refrigerator resided in an rf shielded room. Battery powered current control electronics were also located inside the shielded room and interfaced through fiber optics with a PC situated outside the enclosure. All control lines reaching the device were heavily filtered by discrete element filters at the 1 K stage and mixing chamber as well as copper powder filters attached to the mixing chamber of the refrigerator. All flux bias couplings were weak in order to minimize the dissipation introduced into the qubits from the external environment via the wiring in the refrigerator.

While some effort was made to minimize cross couplings between flux bias controls there was still significant cross talk. We measured the mutual inductance matrix

between lines *in situ* by tracking periodic features (with known flux period Φ_0) that could be attributed to each of the qubits and the coupler. Thus we were able to actively compensate for cross coupling during measurements. The linear crosstalk is avoidable through better design but the nonlinear biasing effects of the coupler's persistent current I_p^b on the qubits [20] cannot be avoided. To calibrate this quantity we suppressed I_c^c of one of the qubits q and then measured the flux state of the second qubit $q' \neq q$ as a function of the coupler bias ϕ_x^b and the latter qubit's bias $\phi_x^{q'}$. The total flux applied to the second qubit is then $\Phi^{q'} = M^{q'b} I_p^b + \Phi_x^{q'}$ and leads to a modulation of the external flux $\Phi_x^{q'}$ required to reach the qubit degeneracy point at $\Phi^{q'} = \Phi_0/2$. Fitting of these data allowed for an experimental determination of β^b as noted above. After performing this calibration, we were able to compensate for all linear and non-linear flux biases.

The effective coupling J in Eq. (1) was measured by mapping the groundstate of the coupled system as a function of ϵ^a and ϵ^c while Δ^a and Δ^c were minimized. In this case Eq. (1) is approximately the classical Ising Hamiltonian, with eigenstates $|ac\rangle = |\uparrow\uparrow\rangle, |\uparrow\downarrow\rangle, |\downarrow\uparrow\rangle, \text{ and } |\downarrow\downarrow\rangle$. However, in the case where there is a large tunnel barrier (high I_p^q , small Δ^q) between the two low lying states of each qubit, the coupled system does not relax to its groundstate on an experimentally accessible timescale. To assist with the relaxation process we employ an annealing procedure in which we first lower the tunnel barriers between the two qubit states by biasing the compound junctions near $\phi_x^{d,e} = \pi$ and then slowly raise the barriers back to their maximum values at $\phi_x^{d,e} = 0$. Thereafter we measure the flux state of the system. Lowering the barriers enhances quantum tunneling and the system is expected to quickly relax to its groundstate. The system remains in the groundstate during the adiabatic raising of the barriers until the effects of tunneling become negligible. The measured flux state is then representative of the groundstate of Eq. (1) at the last instance where tunneling has an appreciable influence. Thus according to Eq. (2) the observed value of J will be determined by particular values of $I_p^a(\phi_x^d)$ and $I_p^c(\phi_x^e)$. The magnitude of these latter two quantities will be inferred from experimental results.

To demonstrate coupler performance we examined the system at three distinct values of the coupler bias ϕ_x^b that corresponded to maximum antiferromagnetic ($\phi_x^b = 0$), zero [$\phi_x^b = \phi_{J=0}^b$ where $\phi_{J=0}^b \in (0, \pi)$] and maximum ferromagnetic ($\phi_x^b = \pi$) coupling. For each fixed value of ϕ_x^b the circuit was subjected to the annealing sequence described above and the resultant flux state of the system was measured. Each measurement was repeated 1,024 times and the probability of finding the system in each possible flux state was determined. The probabilities will be denoted as $P(|\uparrow\uparrow\rangle)$ etc. As an example, Fig. 2

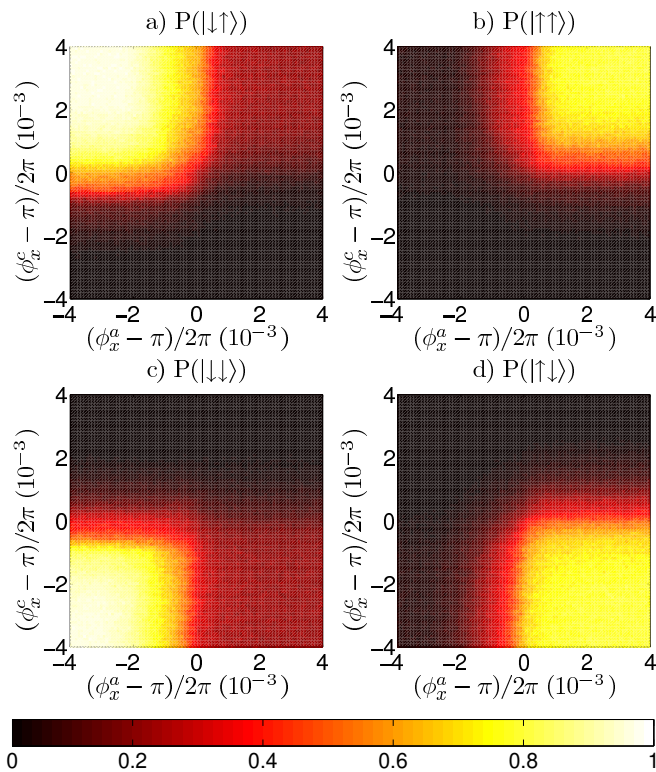


FIG. 2: Sample results for coupler flux bias $\phi_x^b/2\pi = -0.03$. Measured probabilities for each of the four possible flux eigenstates in the small Δ_q limit are shown as indicated.

displays the measured probabilities for $\phi_x^b/2\pi = -0.03$. Note that the flux states observed near the four corners $(\phi_x^a - \pi, \phi_x^c - \pi)/2\pi = (\pm 4, \pm 4) \times 10^{-3}$ agree with those expected from Eq. (1) in the limit $\epsilon^a, \epsilon^c \gg J$. While these results indicate that $P(|\downarrow\uparrow\rangle)$ (Fig. 2a) and $P(|\downarrow\downarrow\rangle)$ (Fig. 2c) exceed 95% at the top left and bottom left corners of their respective plots, it appears that $P(|\uparrow\uparrow\rangle)$ (Fig. 2b) and $P(|\uparrow\downarrow\rangle)$ (Fig. 2d) only reach maximum values $\sim 85\%$. Further investigation revealed that this difference was due to backaction from the readout devices which resulted in a transition from $|i\uparrow\rangle$ to $|i\downarrow\rangle$ approximately 15% of the time.

To generate groundstate stability diagrams we determined which flux state occurs with the highest probability at each point (ϕ_x^a, ϕ_x^c) where the system was probed. The experimentally determined boundaries between adjacent groundstates are denoted as black pixels in Fig. 3. Fig. 3a shows the results for $\phi_x^b/2\pi = -0.03$ in which the regions occupied by the antiferromagnetically aligned groundstates $|\uparrow\downarrow\rangle$ and $|\downarrow\uparrow\rangle$ dominate the groundstate map. Furthermore, one can clearly observe a boundary between these two states which can only occur if $J > 0$ in Eq. (1). Therefore these results demonstrate that our device can provide an *antiferromagnetic qubit-qubit interaction*. Next, for $\phi_x^b/2\pi = 0.30$ (Fig. 3b) our results demonstrate the critical case of *zero coupling* [$J = 0$ in

Eq. (1)]. Note that the flux state of each qubit is independent of the flux applied to the other qubit, thus resulting in the cross structure shown with the fourfold degeneracy point at $(\phi_x^a - \pi, \phi_x^c - \pi) = (0, 0)$. Finally, for $\phi_x^b/2\pi = 0.52$ (Fig. 3c) one observes an enhancement of the regions occupied by the ferromagnetically aligned groundstates $|\downarrow\downarrow\rangle$ and $|\uparrow\uparrow\rangle$ and the generation of a new boundary between them. This feature is present only if $J < 0$ in Eq. (1), thus indicating a *ferromagnetic qubit-qubit interaction*. Ideally this new boundary should have intersected the $J = 0$ fourfold degeneracy point. However, the boundary appears to be translated along both ϕ_x^a and ϕ_x^c by the same amount ($\sim 1 \times 10^{-3}$). This effect must be attributed to a common and symmetric source of flux with respect to the qubits. A plausible explanation is a residual amount of uncompensated flux from the coupler circulating current. However, this in no way undermines the conclusion that this is a demonstration of ferromagnetic coupling between the qubits.

To characterize the strength of the qubit-qubit interaction J we measure either the relative displacement between the $|\downarrow\uparrow\rangle:|\uparrow\uparrow\rangle$ and $|\downarrow\downarrow\rangle:|\uparrow\downarrow\rangle$ boundaries (vertical red lines in Fig. 3) or between the $|\uparrow\uparrow\rangle:|\uparrow\downarrow\rangle$ and $|\uparrow\downarrow\rangle:|\downarrow\downarrow\rangle$ boundaries (horizontal lines). According to Eq. (2) the former should yield a net flux equal to $2|J|/I_p^a$ and the latter equal to $2|J|/I_p^c$. However the observed horizontal and vertical relative displacements are equal to within experimental error for both the ferromagnetic (mean $(0.6 \pm 0.2) \times 10^{-3}$) and antiferromagnetic (mean $(2.0 \pm 0.4) \times 10^{-3}$) cases. As such one must conclude that the qubits and the transformers are reasonably symmetric and one can safely assume $I_p^a \approx I_p^c \equiv I_p^q$. A summary of the measured coupled flux values $J/(I_p^q \Phi_0)$ versus ϕ_x^b is shown in Fig. 4. In addition, we show fits to the form of Eq. (2) using experimental values of $dI_p^b/d\Phi_x^b$ as determined from our measurements of the nonlinear flux bias $M^{qb} I_p^b$ and using I_p^q as a free parameter.

Our results indicate that the observed amount of coupled flux is in reasonable agreement with the theoretical picture presented in Ref. [20] if the qubit persistent currents are on the order of $I_p^q = 0.5 \pm 0.1 \mu\text{A}$ at the last instance during annealing when quantum tunneling has an appreciable influence. These results clearly demonstrate that we have successfully implemented a *sign and magnitude* tunable coupling element between two superconducting flux qubits. While originally designed as a coupling element for a specific superconducting quantum computer processor architecture, this device may prove useful for a variety of superconducting electronics applications, both quantum and classical, where *in situ* tunability is required.

We acknowledge useful discussions with Siyuan Han, Eric Ladizinsky, Jeremy Hilton, Geordie Rose, Alex Tcaciuc and Florin Cioata.

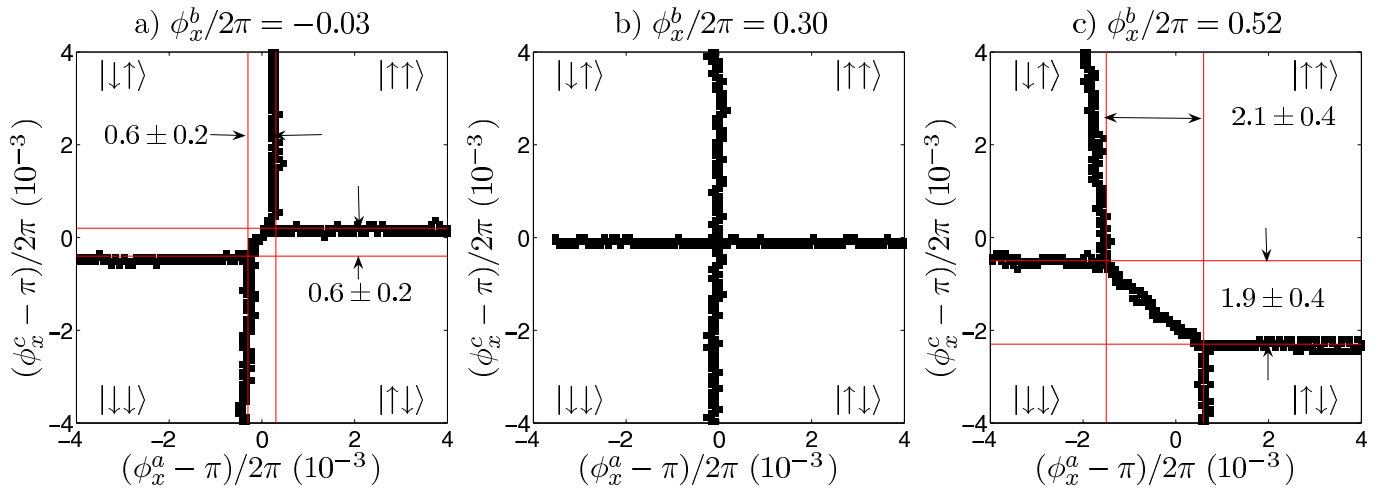


FIG. 3: The experimentally determined groundstate stability diagrams for three different coupler flux biases: a) $\phi_x^b/2\pi = -0.03$ (antiferromagnetic coupling), b) $\phi_x^b/2\pi = 0.30$ (zero coupling) and c) $\phi_x^b/2\pi = 0.52$ (ferromagnetic coupling).

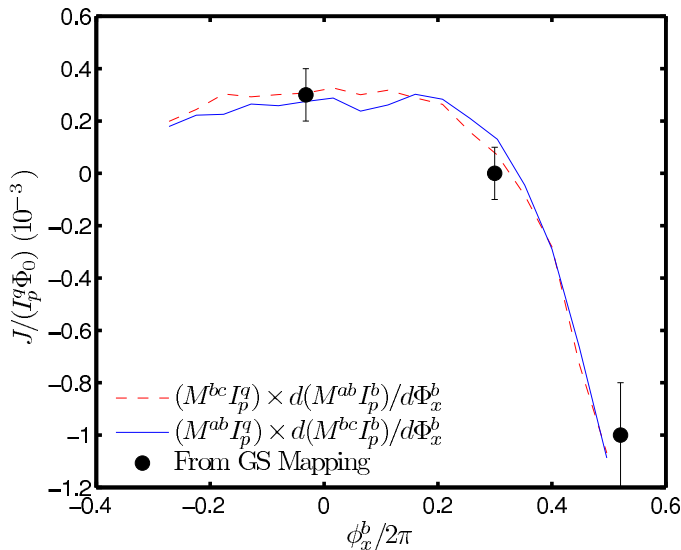


FIG. 4: Coupling strength (in units of coupled flux) versus ϕ_x^b as determined from groundstate mapping. Also shown are plots of the first derivative of the persistent current of the coupler as detected by qubit a (dashed line) and qubit c (solid line) scaled by $M^{ab} I_p^q$ with $I_p^q = 0.5 \pm 0.1 \mu\text{A}$ [see Eq. (2)].

- [3] W. M. Kaminsky, S. Lloyd, and T. P. Orlando (2004), [quant-ph/0403090](#).
- [4] M. R. Garey and D. S. Johnson, *Computers and Intractability, A Guide to the Theory of NP-Completeness* (W. H. Freeman and Company, 1979).
- [5] G. Wendin and V. S. Shumeiko, *Handbook of Theoretical and Computational Nanoscience* (American Scientific Publishers, 2005).
- [6] M. R. Geller, E. J. Pritchett, A. T. Sornborger, and F. K. Wilhelm (2006), [quant-ph/0603224](#).
- [7] M. Devoret, A. Wallraff, and J. Martinis (2004), [cond-mat/0411174](#).
- [8] Y. Makhlin, G. Schön, and A. Shnirman, *Rev. Mod. Phys.* **73**, 357 (2001).
- [9] Thom et al., US patent application publication no. US 2006/0147154 A1 (6 July 2006).
- [10] Maassen van den Brink et al., PCT patent application publication no. WO 2006/066415 A1 (29 June 2006).
- [11] A. J. Leggett and A. Garg, *Phys. Rev. Lett.* **54**, 857 (1985).
- [12] M. F. Bocko, A. M. Herr, and M. J. Feldman, *IEEE Trans. Appl. Supercond.* **7**, 3638 (1997).
- [13] J. R. Friedman, V. Patel, W. Chen, S. K. Tolpygo, and J. E. Lukens, *Nature* **406**, 43 (2000).
- [14] F. Chiarello, P. Carelli, M. G. Castellano, C. Cosmelli, L. Gangemi, R. Leoni, S. Poletto, D. Simeone, and G. Torrioli (2005), [cond-mat/0506663](#).
- [15] S.-X. Li, W. Qiu, Z. Zhou, M. Matheny, W. Chen, J. E. Lukens, and S. Han (2005), [cond-mat/0507008](#).
- [16] S. Han, J. Lapointe, and J. E. Lukens, *Phys. Rev. Lett.* **63** (1989).
- [17] S. Han, J. Lapointe, and J. E. Lukens, *Phys. Rev. B* **46** (1992).
- [18] M. Grajcar, A. Izmalkov, S. H. W. van der Ploeg, S. Linzen, T. Plecenik, T. Wagner, U. Hübner, E. Il'ichev, H.-G. Meyer, A. Yu. Smirnov, P. J. Love, A. Maassen van den Brink, M. H. S. Amin, S. Uchaikin, and A. M. Zagoskin, *Phys. Rev. Lett.* **96**, 047006 (2006).
- [19] B. L. T. Plourde, J. Zhang, K. B. Whaley, F. K. Wilhelm, T. L. Robertson, T. Hime, S. Linzen, P. A. Reichardt, C. E. Wu, and J. Clarke, *Phys. Rev. B* **70**, 140501(R)

* Electronic address: rharris@dwavesys.com

† Currently at Frontier Research System, The Institute of Physical and Chemical Research (RIKEN), Wako-shi 351-0198, Japan; Electronic address: alec@riken.jp

‡ URL: www.dwavesys.com

[1] E. Farhi, J. Goldstone, S. Gutmann, and M. Sipser, *Science* **292**, 472 (2000).

[2] W. M. Kaminsky and S. Lloyd, in *Quantum Computing and Quantum Bits in Mesoscopic Systems*, MQC² (Kluwer Academic, 2003).

- (2004).
- [20] A. Maassen van den Brink, A. J. Berkley, and M. Yalowsky, *New J. Phys.* **7**, 230 (2005).
- [21] S. H. W. van der Ploeg, A. Izmalkov, A. Maassen van den Brink, U. Hübner, M. Grajcar, E. Il'ichev, H.-G. Meyer, and A. M. Zagoskin (2006), [cond-mat/0605588](#).
- [22] M. G. Castellano, F. Chiarello, R. Leoni, D. Simeone, G. Torrioli, C. Cosmelli, and P. Carelli, *Appl. Phys. Lett.* **86**, 152504 (2005).
- [23] A. Maassen van den Brink (2006), [cond-mat/0605398](#).
- [24] V. Zakosarenko, N. Bondarenko, S. H. W. van der Ploeg, A. Izmalkov, S. Linzen, J. Kunert, M. Grajcar, E. Il'ichev, and H.-G. Meyer (2006), (unpublished).
- [25] D. V. Averin, J. R. Friedman, and J. E. Lukens, *Phys. Rev. B* **62**, 11802 (2000).
- [26] C. Cosmelli, P. Carelli, M. G. Castellano, F. Chiarello, R. Leoni, and G. Torrioli, *IEEE Trans. Appl. Supercond.* **11**, 990 (2001).
- [27] C. Cosmelli, F. Sciamanna, M. G. Castellano, R. Leoni, G. Torrioli, P. Carelli, and F. Chiarello, *Appl. Phys. Lett.* **80**, 3150 (2002).